PHYSICAL REVIEW E VOLUME 57, NUMBER 2 FEBRUARY 1998

Crack dynamics and crack surfaces in elastic beam lattices

Jan Åström,[1] Mikko Alava,[2,3] and Jussi Timonen[1]
[1]*Department of Physics, University of Jyväskylä, P.O. Box 35, FIN-40351 Jyväskylä, Finland*
[2]*NORDITA, Blegdamsvej 17, DK-2100 Copenhagen, Denmark*
[3]*Helsinki University of Technology, Laboratory of Physics, P.O. Box 1100, FIN-02015 HUT, Finland*
(Received 24 September 1997)

The dynamics of propagating cracks is analyzed in elastic two-dimensional lattices of beams. At early times, inertia effects and static stress enhancement combine so that the crack-tip velocity is found to behave as $t^{1/7}$. At late times a minimal crack-tip model reproduces the numerical simulation results. With no disorder and for fast loading, a ''mirror-mist-mirror'' crack-surface pattern emerges. Introduction of disorder leads, however, to the formation of the ''mirror-mist-hackle''–type interface typical in many experimental situations. [S1063-651X(98)50902-6]

PACS number(s): 03.20.+i, 62.20.Mk, 46.30.Nz

By far the simplest way to break a piece of glass is to apply tensile stress to its surface (e.g., by bending it). An imperfection at the surface leads to stress concentration, and for a high enough load a crack appears. As the crack propagates it has been observed to create a pattern on the crack surface known as the mirror-mist-hackle [1–3]. The mechanisms leading to this pattern are not fully understood, and it may look slightly different in different materials. Combining a few qualitative descriptions [1–3] gives the following picture: At first the crack leaves behind a more or less smooth surface (the mirror). As the velocity of the crack tip increases, the crack surface roughens ''visibly,'' and close to but below a half of the velocity of transverse elastic waves, sidebranching becomes so dense that the surface looks misty. Further increase of roughness with growing crack velocity leads to simultaneous propagation of several macroscopic cracks. As these cracks merge, the surface of the final crack is usually diverted away from the initial crack plane, which results in the hackle. If the crack continues to propagate, it may finally bifurcate, and if the stress becomes very high, the glass will be shattered [2,3].

The dynamic propagation of cracks in brittle solids has recently attracted revived interest. This topic was introduced by Yoffe [4], who demonstrated the instability of propagating cracks. The experimental fact that crack velocities seem to be limited to a fraction of the Rayleigh velocity, has induced several studies on this topic [5–16]. Experiments and the corresponding theoretical models have addressed phenomena such as crack branching [5–8], oscillation of the crack-tip velocity [7,9,10], and spatial crack oscillations [11].

In this paper we study the velocity of a propagating crack in a triangular lattice of beams [17]. This model, if there is no disorder, has a divergent crack-tip velocity, and produces a mirror-mist-*mirror* pattern as external strain is increased. If disorder is introduced, a mirror-mist-hackle pattern is found. The crack velocity is found to result from a combination of crack-tip inertia effects and static-limit fracture-mechanics effects. The specific nature of the beam lattice seems to play a role in the formation of crack-surface topology and in the crack velocity when it is determined by local dynamics only.

The beam-lattice model which we analyze, represents a discretization of a brittle two-dimensional solid obeying ''Cosserat elasticity'' [18,19]. This means that large scale rotations are possible. We use a triangular lattice in which the lattice bonds are slender elastic beams with a square cross-section w^2, length l, and Young's modulus E. The stiffness matrix of a beam is given by

$$K_l=\begin{pmatrix} \frac{EA}{l} & 0 & 0 & \frac{-EA}{l} & 0 & 0 \\ 0 & \frac{12EI}{l^3} & \frac{6EI}{l^2} & 0 & \frac{-12EI}{l^3} & \frac{6EI}{l^2} \\ 0 & \frac{6EI}{l^2} & \frac{4EI}{l} & 0 & \frac{-6EI}{l^2} & \frac{2EI}{l} \\ \frac{-EA}{l} & 0 & 0 & \frac{EA}{l} & 0 & 0 \\ 0 & \frac{-12EI}{l^3} & \frac{-6EI}{l^2} & 0 & \frac{12EI}{l^3} & \frac{-6EI}{l^2} \\ 0 & \frac{6EI}{l^2} & \frac{4EI}{l} & 0 & \frac{-6EI}{l^2} & \frac{2EI}{l} \end{pmatrix},$$

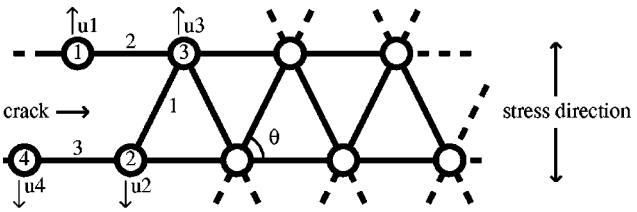

FIG. 1. The local geometry of a triangular beam lattice close to a crack tip. The sites and bonds are numbered, and the directions of displacements u_1, u_2, u_3 are indicated.

where $A=w^2$ and the moment of inertia is $I=w^4/12$. Inertia is introduced in the lattice by having masses m (moment of inertia i) on the lattice sites, while the beams are assumed massless. The boundary conditions we impose are such that a strain $[\epsilon(t)]$ is applied in the vertical y direction (i.e., perpendicular to one of the principal bond directions) by constraining the sites at the top and bottom of the lattice to move a distance up and down, respectively. The sites at the left and right edges are only allowed to move in the y direction to avoid a global Poisson contraction of the lattice. (The results presented in this paper can be compared to those reported for different boundary conditions in Ref. [8].) To create a notch, which can then act as a seed for a crack, a number of bonds $N_{rem}\sim 10$ in the middle of the left edge are removed at $t=0$. The other bonds are assumed to break instantly and irreversibly if their strain exceeds a threshold value, which in our case is taken to be a constant (ϵ_b). The dynamics of the lattice is determined by a discrete form of Newton's equations of motion including a small viscose dissipation term (damping coefficient c) and with zero initial velocities. The lattice model is described in more detail in Refs. [8,20]. Simulations for a constant strain-increase rate, and for a strain that is constant after crack propagation begins, have been performed. The strain rate was of the order $0.01\epsilon_b$, which is several orders of magnitude less than the sound velocity. Disorder is introduced in the lattice by assigning random Young's moduli (E_i) to the lattice bonds. The values of E_i are taken from the distribution $E_i=E_0(1+e\,\delta_i)$, where e is the ''strength'' of the disorder, and $\delta_i\in[-0.5,0.5]$ is a stochastic variable. The specific values of the parameters used in the simulations are given below.

We first consider the crack velocity analytically within a ''minimal'' model [16]. The result will then be extended to the regime of slow crack propagation in the initial phase and compared to numerical simulations. In Fig. 1 we show the lattice in the neighborhood of a crack tip. A crack is propagating from the left, and stress is applied in the vertical direction. We first study the case in which the externally applied strain (ϵ) is close to the failure threshold (ϵ_b) in the diagonal bonds of the lattice (i.e., the bonds that are not horizontal in Fig. 1). In this case only a small distortion around the crack tip is needed to break the next bond, which means that the crack will propagate fast. Breaking of a bond at the crack tip induces a net force on the sites numbered 1 and 2 in the figure. These sites will therefore, as long as the force applied on them can be considered constant, undergo constant acceleration. The crack will propagate a half of a lattice unit when bond 1 breaks. This happens when $u2+u3=(\epsilon_b-\epsilon)l\,\sin\theta$, where l is the bond length and θ is the in-plane angle of the diagonal bonds; $u2$ and $u3$ are defined in Fig. 1. Notice that $u2$ and $u3$ are only the displacements of the sites due to the crack propagation. The slow displacements induced by the external strain are not included in them. The net force on bond 3 results from the bending of bond 2. When the external strain is close to the failure threshold, all displacements around the crack tip are small, and, therefore, the net force on site 3 is negligible as compared to the force on site 2. The latter force (F) is given by

$$F=\frac{Ew^2}{l}\epsilon l\,\sin\,\theta[\sin^2\,\theta+(w/l)^2\,\cos^2\,\theta], \tag{1}$$

where Ew^2/l is the axial stiffness of a beam. Newton's equation of motion gives simply

$$u2=\frac{Ft^2}{2m} \tag{2}$$

for the displacement $u2$. We have assumed that $t=0$ when the bond between sites 1 and 2 breaks. Since $u3\approx 0$ for ϵ close to ϵ_b (i.e., large ϵ), we obtain the crack-tip velocity in the form

$$v(\epsilon)=l/2\left[\frac{2ml(\epsilon_b-\epsilon)/\epsilon}{Ew^2[\sin^2\,\theta+(w/l)^2\,\cos^2\,\theta]}\right]^{-0.5}. \tag{3}$$

This equation implies that the crack-tip velocity diverges as $(\epsilon_b-\epsilon)^{-0.5}$ when $\epsilon\rightarrow\epsilon_b$. Strictly speaking there are also horizontal displacements and angular rotations of the sites, but these do not affect much the crack velocity, which is confirmed by the simulations results below. Notice that Eq. (3) was derived under the assumption of ''large'' strains, which is particularly appropriate for overloading, or for cases in which the available elastic energy exceeds the Griffith's energy.

For lower strains we have to consider the crack-tip dynamics to the next order, in which the force resulting from bending of the horizontal bonds that are closest to the crack tip, i.e., bonds 2 and 3 in Fig. 1, has to be taken into account. If T is the (constant) time between two consecutive bond breakings at the crack tip, we can calculate the displacements of sites 1 and 4 in the same way as above. Then we obtain the force on sites 2 and 3 through bending of bonds 2 and 3. The total displacements u_2 and u_3 are then given by

$$u_2=\frac{GF(5T^2t^2/2+Tt^3+t^4/6)}{2m^2}+\frac{Ft^2}{2m}, \tag{4}$$

$$u_3=\frac{GF(T^2t^2/2+Tt^3/3+t^4/6)}{2m^2}, \tag{5}$$

where $G=Ew^4/l^3$ is the bending stiffness of the bonds. Bond 1 will break when $t=T$. Using the breaking criterion above and solving for T gives us again the crack-tip velocity

$$v(\epsilon)=l/2\left[\frac{\sqrt{\frac{f^2}{4m^2}+\frac{28Gf\epsilon'}{3m^2}}-\frac{f}{2m}}{\frac{14Gf}{3m^2}}\right]^{-0.5}, \tag{6}$$

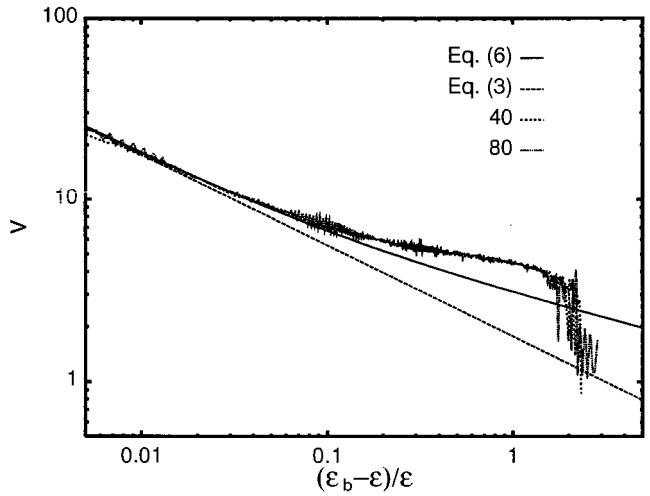

FIG. 2. The crack-tip velocity v as a function of $(\epsilon_b-\epsilon)/\epsilon$ for lattices of size 40×200 and 80×200, with $E_0=1.0$, $w=1.0$, $l=1.15$, and $m=0.05$. The lines are given by Eqs. (3) and (6).

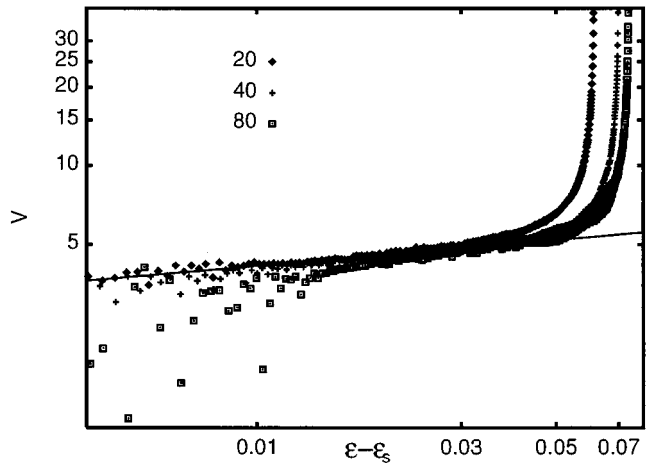

FIG. 3. The crack-tip velocity v as a function of $(\epsilon-\epsilon_s)$ for the same lattice as in Fig. 2. The line is given by Eq. (7).

where $\epsilon'=(\epsilon_b-\epsilon)/\epsilon$, and $f=Ew^2[\sin^2\theta+(w/l)^2\cos^2\theta]/l$. Notice that this equation gives Eq. (3) in the limit $\epsilon'\to0$.

When the external strain is close to the failure threshold of the diagonal bonds, as above, the crack will propagate fast, and there will not be time for stress relaxation in the neighborhood of the crack tip. If we would try to use Eq. (6) to determine the crack-tip velocity for small external strains (i.e., large ϵ'), we would obtain $v(\epsilon)\propto\epsilon^{0.25}$. However, for ϵ small, the crack will initially propagate slowly, and there will appear stress enhancement around the crack tip just as in the static case. The static or quasistatic stress relaxation around a narrow crack of length L produces a stress enhancement at a sharp tip (ϵ_t) of the form $\epsilon_t\propto\epsilon\sqrt{L}$ [1]. By combining the two scaling expressions, $\epsilon_t\propto\epsilon\sqrt{L}$, $v\propto\epsilon_t^{0.25}$, with the fact that the crack-tip velocity is defined by $v=dL/dt$, we can estimate the behavior of the crack-tip velocity at small strains. If the crack begins to propagate with $\epsilon=\epsilon_s$ at $t=t_0$, the crack velocity is given by

$$v(t)\propto\epsilon_s^{2/7}(t-t_0)^{1/7}. \tag{7}$$

Notice that this equation holds only for ϵ just above ϵ_s.

We first tested Eqs. (3) and (6) using the simulation model. We determined the crack-tip velocity in lattices of size 40×200 and 80×200, with $E=1.0$, $w=1.0$, $l=1.15$, and $m=0.05$. The external strain was increased from zero up to ϵ_b, and the crack-tip velocity was computed at each bond failure. The results are shown in Fig. 2 together with those given by Eqs. (3) and (6). For large strains [i.e. for $(\epsilon_b-\epsilon)/\epsilon\leqslant0.02$], Eqs. (3) and (6) both give the correct velocity, while Eq. (6) gives, as expected, a somewhat better result for small strains. For $(\epsilon_b-\epsilon)/\epsilon\geqslant0.2$ the simple approach leading to Eqs. (3) and (6) fails. Stress enhancement around the crack tip is now important, and thus the velocity is satisfactorily predicted by Eq. (7) (cf. Fig. 3). Notice also the system-size dependent cross over to local crack-tip dynamics.

In the case of constant external strain we found that, if the strain was high enough for the crack to propagate, the crack velocity remained constant throughout the entire simulation, except for a short initial phase. Moreover, the velocity for a particular strain was exactly the same as that for dynamic boundary conditions at the time when the dynamic strain was similar to the constant strain.

While one may find the behavior of the crack-tip velocity by local considerations supplemented with static fracture mechanics, phenomena like tip splitting or crack branching and surface roughening are at present only accessible by computer simulations. Using the same parameters as in Figs. 2 and 3, and by increasing the external strain from zero up to ϵ_b, the crack pattern of Fig. 4A is obtained. In the very beginning of crack propagation, it propagates slowly and the situation is very much like in the quasistatic case. The crack propagates straightforward with no side branches, and a mirror region is formed. When dynamical effects first become important, the external strain is still quite far from ϵ_b. This means that bending deformations of the horizontal bonds are still quite large [cf. Eq. (6)]. Breaking of bonds by bending leads to the formation of large sidebranches [6–8]. These sidebranches form the mist region. When ϵ approaches ϵ_b, bending is no longer important, and a mirror region reappears. At the same time the crack velocity increases without bounds. This is in contrast with experiments, in which the hackle region appears and the velocity is limited to a fraction of the Rayleigh velocity [21], unless the stress becomes so high that the whole body is shattered. In our case the reap-

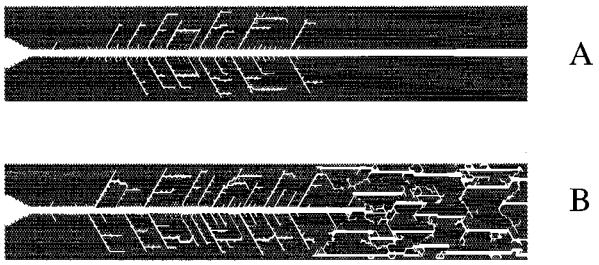

FIG. 4. Crack patterns formed in a lattice of size 40×120, with $E_0=1.0$, $w=1.0$, $l=1.15$, $m=0.05$, $i=0.1$, $c=0.02$, $t_0=50$, and $\epsilon_b=0.06$. A, $e=0.0$ and B, $e=0.1$.

pearance of the mirror seems to result from the crack propagating in a ''soft'' direction of a beam lattice.

It has been suggested that branching is the mechanism that restricts the crack-tip velocity to a fraction of its theoretical value [5]. Velocity fluctuations typical of the branch-forming region can be seen in Figs. 2 and 3. There are, however, no visible signs of a reduced crack-tip velocity in this region. Fluctuations are rather sensitive to the choice of lattice parameters (like the moment of inertia of the sites and the width of the beam elements), which means that there might be [7,8] a range of parameter values for which the branches do affect the velocity. We did simulations also for other parameter values but found no effect on the velocity. The branches always seemed to form at least a few bond lengths behind the crack tip. This is consistent with the results of Refs. [22], in which branching was shown not to be connected with velocity fluctuations.

In contrast with the ordered case above, the hackle region will appear if disorder is introduced in the model. In Fig. 4B we use the same lattice as in Fig. 4A but now the disorder strength is $e=0.1$. When the external strain reaches a high enough value, macroscopic cracks begin to form ahead and on the sides of the main crack. This is analogous to *static* crack propagation in two-dimensional disordered media [23]. As these cracks merge, the final crack will deviate from the initial crack plain and a rough crack surface is formed. The crack-tip velocity is, of course, strongly affected by disorder in the hackle region. It is difficult, however, to determine a unique velocity in this region as several cracks propagate simultaneously. In the mirror and mist regions there was no visible effect of disorder on the crack-tip velocity.

In summary, we have presented a simple minimal crack tip analysis of the velocity of a crack as a function of external strain. This is sufficient for understanding the acceleration of the crack tip in an elastic beam lattice. As long as a staticlike stress enhancement around the tip is important, the crack will accelerate as $t^{1/7}$. There is then a crossover to strictly local behavior, dictated by the constitutive laws and inertia. If there is no disorder in the lattice, a mirror-mist-mirror pattern is formed on the crack surface with increasing external strain. Introducing disorder in the model is sufficient for the experimentally observed mirror-mist-hackel pattern to appear. This indicates that microscopic randomness such as vacancies and microcracks are important in the roughening and dynamics of cracks. This is expected to be found also for ''slow'' fracture [24] in which it is the intrinsic disorder which seems to lead to the roughening of crack interfaces.

[1] H. J. Herrmann, in *Statistical Models for the Fracture of Disordered Media*, edited by H. J. Herrmann and S. Roux (North Holland, Amsterdam, 1990).

[2] J. J. Mecholsky, in *Fractography of Glass*, edited by R. C. Bradt and R. E. Tassler (Plenum Press, New York, 1994).

[3] E. Guilloteau, H. Arribart, and F. Creuzet, in *Fracture—Instability Dynamics, Scaling and Ductile/Brittle Behavior*, edited by R. B. Selinger, J. Mecholasky, E. R. Fuller, Jr., and A. Carlsson Material Research Society Symposium Proceedings Vol. 409 (MRS, Pittsburgh, 1996), p. 365.

[4] E. H. Yoffe, Philos. Mag. **42**, 739 (1951).

[5] E. Sharon, S. P. Gross, and J. Fineberg, Phys. Rev. Lett. **74**, 5096 (1995).

[6] M. Marder and X. Liu, Phys. Rev. Lett. **71**, 2417 (1993).

[7] P. Heino and K. Kaski, Phys. Rev. B **54**, 6150 (1996).

[8] J. Åström and J. Timonen, Phys. Rev. B **54**, 9585 (1996).

[9] J. Fineberg, S. P. Gross, M. Marder, and H. L. Swinney, Phys. Rev. Lett. **67**, 457 (1992).

[10] E. Sharon, S. P. Gross, and J. Fineberg, Phys. Rev. Lett. **74**, 5096 (1995).

[11] F. Abraham, D. Brodbeck, R. A. Rafey, and W. E. Rudge, Phys. Rev. Lett. **73**, 272 (1994).

[12] S. P. Gross, J. Fineberg, M. Marder, W. D. McCormick, and H. L. Swinney, Phys. Rev. Lett. **71**, 3162 (1993).

[13] E. Sharon, S. P. Gross, and J. Fineberg, Phys. Rev. Lett. **76**, 2117 (1996).

[14] J. S. Langer, Phys. Rev. Lett. **70**, 3592 (1993).

[15] E. S. C. Ching, J. S. Langer, and H. Nakanishi, Phys. Rev. Lett. **76**, 1087 (1996).

[16] B. L. Holian, R. Blumenfeld, and P. Gumbsch, Phys. Rev. Lett. **78**, 78 (1997).

[17] H. Furukawa, Prog. Theor. Phys. **90**, 949 (1993).

[18] W. Nowacki, *Theory of Micropolar Elasticity* (Springer-Verlag, Udine, 1972).

[19] S. Roux, in (Ref. [1]).

[20] J. Åström, M. Kellomäki, M. Alava, and J. Timonen, Phys. Rev. E **56**, 6042 (1997).

[21] L. B. Freund, *Dynamic Fracture Mechanics* (Cambridge Univ. Press, New York, 1985).

[22] J. F. Boudet, S. Ciliberto, and V. Steinberg, J. Phys. (France) II **6**, 1493 (1996); J. F. Boudet, V. Steinberg, and S. Ciliberto, Europhys. Lett. **30**, 337 (1995).

[23] V. I. Räisänen, E. T. Seppälä, M. J. Alava, and P. M. Duxbury (unpublished).

[24] P. Daugier, B. Nghiem, E. Bouchaud, and F. Creuzet, Phys. Rev. Lett. **78**, 1062 (1997).